Eksplorium
Volume 46 No. 1, May 2025: 27–46

p-ISSN 0854-1418
e-ISSN 2503-426X

Evaluation of Geothermal Prospects in The Patuha Field Based on Derivative Analysis and 3D Inversion of Gravity Anomaly

Soraya Tiana Dewi[1], Muh Sarkowi[1], Rahmat Catur Wibowo[2*]
[1]Geophysical Engineering Department, Universitas Lampung,
Prof. Sumantri Brojonegoro St., No. 1, Bandar Lampung, Lampung, 35145, Indonesia.
[2]Geological Engineering Department, Universitas Lampung,
Prof. Sumantri Brojonegoro St., No. 1, Bandar Lampung, Lampung, 35145, Indonesia.
*E-mail: rahmat.caturwibowo@eng.unila.ac.id

Article received: 5 April 2025, revised: 23 May 2025, accepted: 31 May 2025
DOI: 10.55981/eksplorium.2025.11327

ABSTRACT

The Patuha geothermal field has the potential to be developed as a source of energy for power generation. This study was conducted to evaluate the Patuha geothermal system based on Global Gravity Model Plus Gravity data. The study refers to the Bouguer Anomaly value, which is the difference between the observed gravity value (g_{obs}) and the theoretical gravitational value (g_n), or the sum of corrections applied to the gravity measurement. This difference reflects variations in mass density between the survey area and its surroundings, occurring in both lateral and vertical directions. Derivative analysis and 3D inversion of gravity anomalies are used to identify the presence of faults, reservoir prospects, cap rocks, and heat sources. The Complete Bouguer Anomaly map displays decreasing values from southwest to northeast. The high anomaly coincides with Mount Patuha, indicating that this feature may become the heat source. The 3D inversion of the gravity anomaly yielded a density range of 2 g/cm³ to 3 g/cm³. The reservoir prospect is controlled by the graben structure and is located in the Ciwidey Crater. It has a density of 2.5 g/cc, with an area of 130 km^2, located at a depth of 2200 meters above MSL to 700 meters below MSL. Cap rock crosses along the Cibuni Crater, White Crater, and Ciwidey Crater with a density of 2.66 g/cc at a depth of 2300 meters to 800 meters above MSL. The heat source is shallow and originates from Mount Patuha, with a density of 3 g/cc at a depth of 1500 meters above MSL and 4600 meters below MSL.

Keywords: Patuha, geothermal, anomaly, structure

INTRODUCTION

Geothermal energy, a natural heat source from within the Earth, can be extracted and converted into electricity [2]. The formation of a geothermal system requires heat sources (such as hot rocks or fluids), permeable reservoir rocks with high porosity, and impermeable cap rocks. The utilization of geothermal energy involves exploration or drilling activities and the injection of fluids to sustain thermal energy output [1]. PT Geo Dipa Energi (Persero), the permit holder for the Patuha area, operates the Patuha 1 geothermal power plant (PLTP) with a capacity of 55 MW, including 17 MWe of probable reserves, 210 MWe of estimated reserves, and 190 MWe of proven reserves, contributing to a total installed capacity of 282 MW as of 2021 [3]. The Patuha geothermal field is considered one of the most promising for energy development due to its location on a volcanic plateau composed of Pliocene to Quaternary pyroclastic flow and andesite rocks that radiometrically dated to between 0.12 and 1.25 million years [4].Its tectonic setting is on the volcanic arc generated by the subduction of the Indo-Australian Plate beneath the Eurasian Plate in the Java Trench. Although there is no recorded eruption history,

aerial imagery has identified several volcanic centers (vents) [4].

The gravity method is a geophysical technique used to characterize subsurface geological conditions by analyzing variations in rock density. This method plays a key role in identifying geothermal system components such as heat sources, reservoirs, and cap rocks [5] and in defining reservoir geometry and controlling geological structures [6]. Geothermal-related density variations serve as the basis for gravity investigations, since the presence and accumulation of a heat source beneath the Earth's surface results in a density contrast with the surrounding rock mass [7].

GGMplus 2013 satellite gravity data, derived from the Global Gravity Model, offers ultra-high resolution with a 200-meter north-south grid spacing [8]. It enables a detailed depiction of the gravitational field and enhances the ability to model subsurface structures by estimating the depth, density, and geometric shape of gravity anomalies [9].

This study was conducted to evaluate the faults, location of reservoir prospects and boundaries, cap rocks, and heat sources of the Patuha Geothermal Field. This study was also supported by magnetotelluric (MT) data in a journal entitled Integrated Analysis of Magnetotelluric and Gravity Data to Describe Reservoir Zones in the Patuha Geothermal Field, West Java [10] to identify reservoir prospects, reservoir boundaries, cap rock distributions, and heat source zones, ultimately contributing to the evaluation of geothermal potential.

GEOLOGY

The research area is in the Patuha geothermal prospect area, located in Bandung City and West Bandung, West Java Province (Figure 1). The research area is 15 km x 15 km wide, located at coordinates 760000–775000 mE and 9200000–9215000 mN, which corresponds to the Universal Transverse Mercator (UTM) zone 48S.

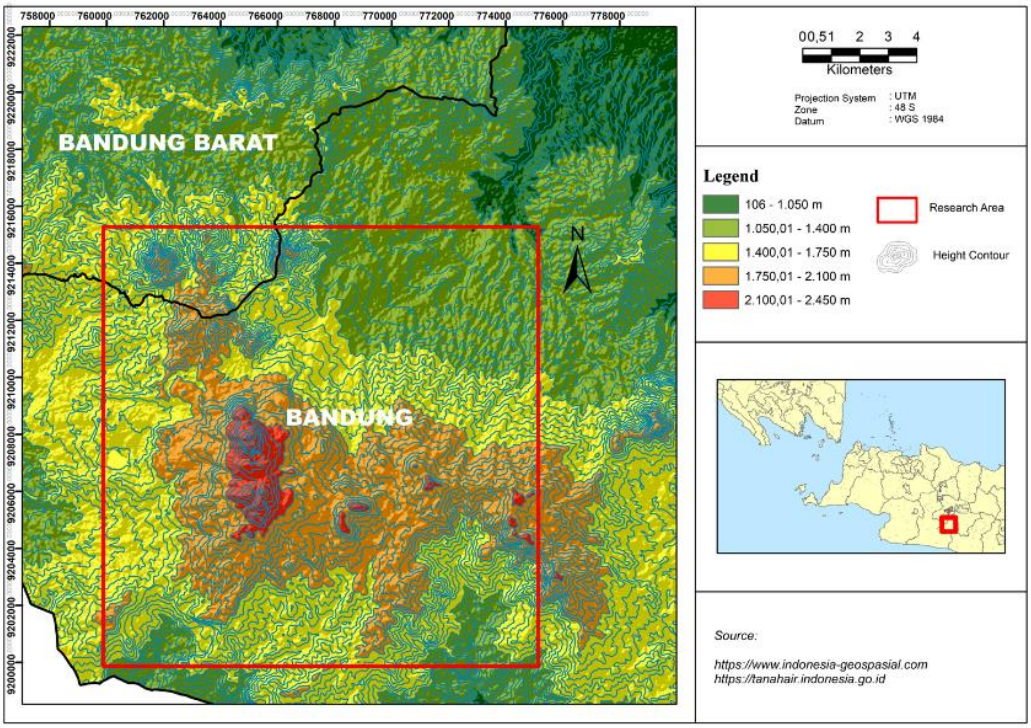

Figure 1. Research location map [14]

p-ISSN 0854-1418
e-ISSN 2503-426X

The research area is composed of the Terumbu Limestone Formation (QI), Lava of Mount Patuha (Qv2), Sindangkerta Member (Tmcs), Tufa and Breksi Member (Tpv1), as seen in Figure 2. The formation that dominates the research area is the Terumbu Limestone Formation (QI). The youngest volcanic activity zone consists of domes and volcanic craters. Some domes have a slightly silicic composition (dacite or rhyodacitic), such as on Mount Urug and Mount South Patuha. Furthermore, thin lava flows form morphologies that can indicate the direction of flow from the northern tip of Mount Patuha, consisting of basaltic andesite and basaltic compositions. The western part of Mount Patuha consists of thicker lava and silicic compositions [15].

The geothermal energy of the Patuha area is associated with a volcanic axis, as evidenced by the presence of late-stage volcanic centers concentrated along a west–northwest trending zone. The main structural pattern in West Java generally consists of the southwest–northeast-trending Cimandiri Fault, as well as the Rajamandala thrust fault. The fault directions follow the pattern of the Limestone Arc, commonly referred to as the Meratus direction [16]. The location of the heat source and magma emergence in the Patuha geothermal system is controlled by a west–northwest trending structural zone. Fractures related to this structure likely control the distribution of volcanic vents in the Patuha reservoir. North–south trending faults correspond to alignments of volcanic vents at Mount Patuha, South Patuha, Kawah Putih, and other southern mountain peaks. Another fault trending northeast–southwest is indicated by topographic alignments in the southeastern part of the field [15].

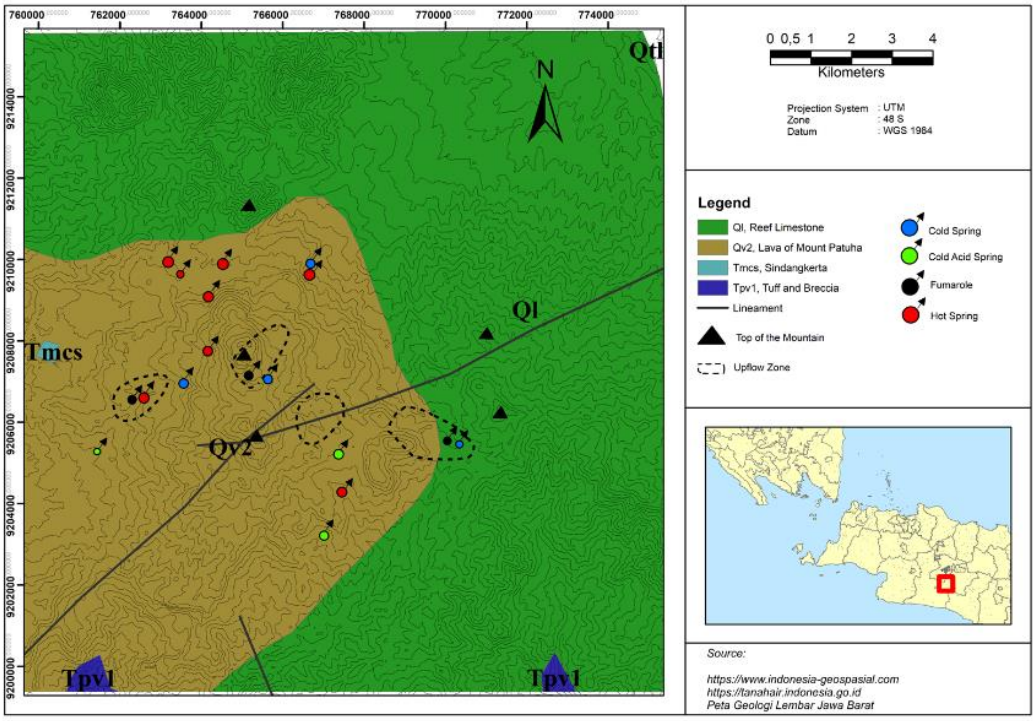

Figure 2. Geological map of the research area [17], [18]

Manifestations in the Patuha Field are in the form of hot springs, fumaroles, and cold gas output. Fumarole manifestations are found in the Cibuni Crater, White Crater, and Ciwidey Crater. Therefore, it can be inferred that a steam flow is present below the surface, which is influenced by the permeable zone [19]. The Patuha Field is composed of several main components, including a steam reservoir located above the upflow zone, a magnetic plume, a water zone, an estimated direction of fluid movement, and an estimated subsurface temperature. The water of Kawah Putih Lake is the result of the interaction of surface water with the steam [20]. It can be concluded that the Patuha geothermal reservoir is a two-phase reservoir dominated by steam and controlled by a structure with an area of 20 km [19] (Figure 3).

There is a major fault structure that intersects the Patuha area (Figure 4), which is the Cikalong Fault (thrust fault). The location of the heat source and the emergence of magma in the Patuha geothermal system are controlled by the west-northwest structural zone. The related fractures likely control the priming of the volcanic vent in the Patuha reservoir. The north-south fault is the lineament of volcanic vents on Mount Patuha, South Mount Patuha, Kawah Putih, and the southern mountain peaks. The topographic lineament in the southeastern area of the field indicates another northeast-southwest fault [15].

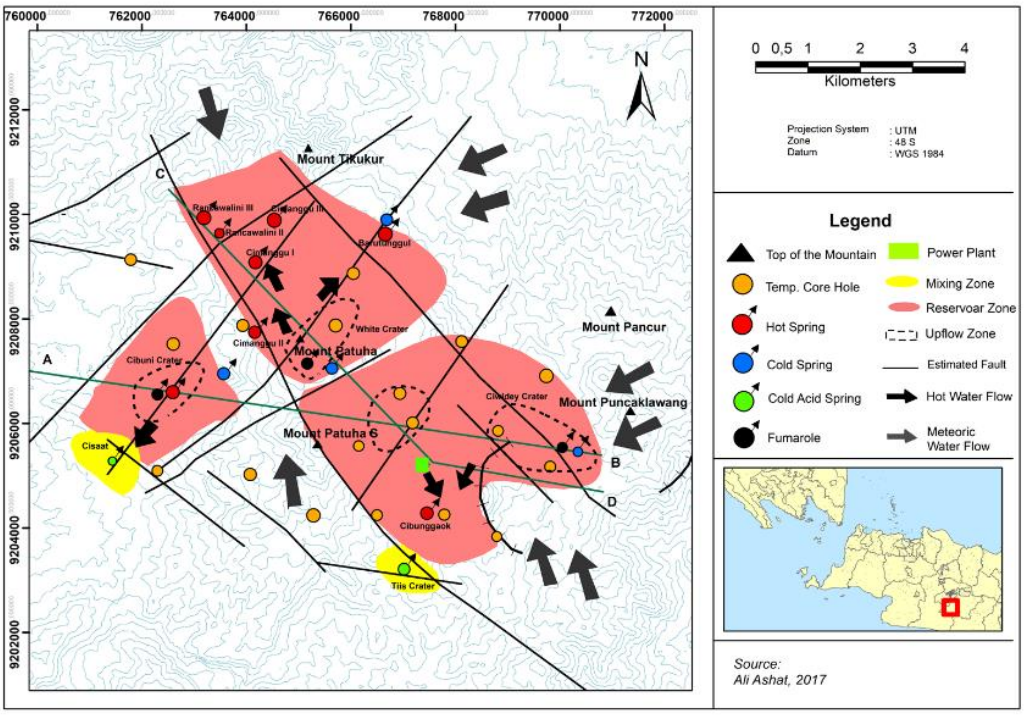

Figure 3. Map of the location of the Patuha geothermal area (modified from [21])

p-ISSN 0854-1418
e-ISSN 2503-426X

Figure 4. West Java structural pattern [22]

METHODOLOGY

This study commenced with a comprehensive literature review to guide the identification of the study area, drawing upon credible sources such as geological information, geothermal prospect data, and magnetotelluric (MT) modeling. Satellite-based gravity data were acquired from the Global Gravity Model Plus (GGMPlus) 2013, comprising 6,120 data points across an area of 15 × 15 km². Standard gravity corrections, including free-air correction, Bouguer correction, and terrain correction, were applied to minimize the influence of external gravitational effects. Average surface density was estimated using the Parasnis and Nettleton methods. Upon deriving the complete Bouguer anomaly, spectral analysis was conducted to determine the depth separation between regional and residual anomalies. Subsequently, a moving average filter was employed to define the appropriate window width. Residual anomaly data were further analyzed through derivative methods and subjected to 3D inversion modeling to delineate fault structures and assess geothermal potential in the Patuha area. The geothermal prospect was then evaluated by comparing the gravity inversion results with existing literature MT modeling interpretations (Figure 5).

Complete Bouguer Anomaly (CBA)

The Complete Bouguer Anomaly (CBA) value was obtained by performing the gravity data correction stages. The gravity data corrections (free air correction, Bouguer correction, and terrain correction) are performed before interpretation because gravity values vary at each location. Differences in gravity value readings are influenced by topographic variations (height variations, tidal latitudes, density variations, and shocks to the instrument springs) [11]. The Free Air Correction is used to obtain the value of absolute gravity readings at an observation point, representing the difference in gravity measured at mean sea level and the gravity value measured at a height of *h* meters above it, assuming there is no intervening rock mass between the two points [12].

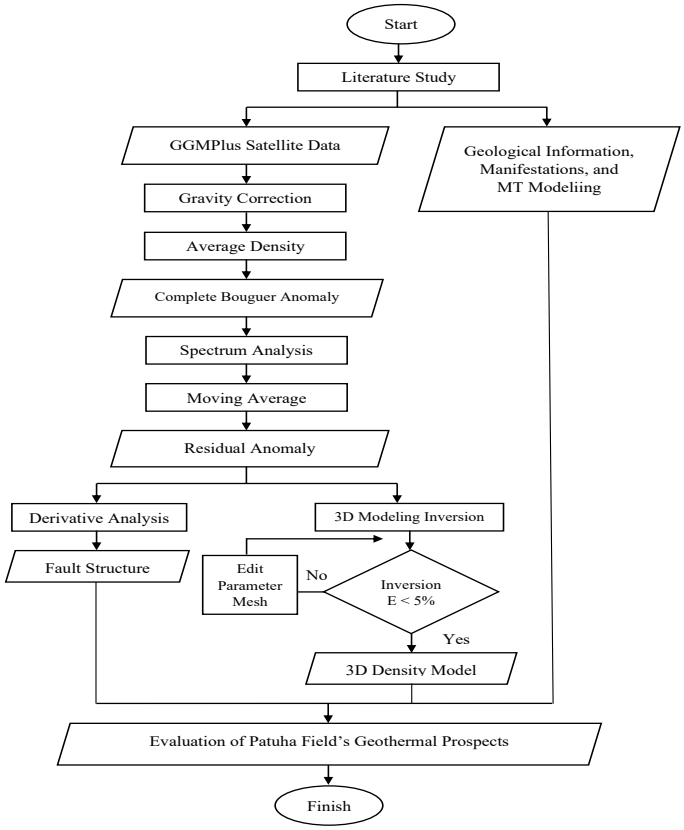

Figure 5. Data processing flow diagram

The Bouguer Correction is applied to eliminate the effects of elevation differences while still accounting for the mass beneath the observation point. The principle involves calculating the gravitational attraction exerted by rocks with a density (ρ) and a thickness (h) [13]. Terrain correction is applied in areas with hilly topography. In contrast, in regions with relatively flat terrain, corrections are typically performed only up to the level of obtaining the simple Bouguer anomaly. The presence of nearby hills and valleys generates gravitational attraction due to the mass center of the hills or the mass deficiency represented by the valleys [12].

To get the CBA value, the simple Bouguer anomaly value was added to the terrain correction value obtained from the calculation. After receiving the CBA value, the next step was to perform gridding to create a Bouguer anomaly map.

Spectrum Analysis

The spectrum analysis process estimates the depth of the regional and residual areas by knowing the frequency content of the data. The principle of spectrum analysis is the Fourier transform, which changes the distance domain to the frequency domain. Regional anomalies have a low frequency, while residual anomalies have a high frequency. The Fourier transform equation of the gravity anomaly force is [23]:

$$F(g_z) = 2\pi\gamma\mu e^{|k|(z_0 - z)} \quad (1)$$

where:

(g_z) : gravity anomaly
μ : mass density anomaly
γ : gravity constant
$\left(\frac{\partial}{\partial z}\right)$: partial derivative with variable z
$\left(\frac{\partial}{\partial z}\ \frac{1}{r}\right)$: partial derivative of $\frac{1}{r}$ variable z

p-ISSN 0854-1418
e-ISSN 2503-426X

In this study, spectrum analysis was performed using four trajectories, and a Fourier transform was then carried out using Numeri software. Next, calculations were performed on Excel software to obtain the wave number (K) and Ln A values. Calculations of K and Ln A values were performed to get the window width value. The next stage was to filter anomalous data by inputting the window width value.

Separation of Regional and Residual Anomaly

The Bouguer anomaly data is still affected by sources on a regional (deep) and residual (shallow) scale. The anomaly separation method employed in this study utilized a moving average filter within the Surfer 13 software. The target of this study is to analyze the subsurface structure caused by shallow anomaly sources. Hence, residual anomalies were needed for the structure interpretation process. The moving average is a technique for averaging anomaly values, with properties similar to a low-pass filter, which passes low frequencies (regional anomalies). At the same time, residual anomalies were obtained by subtracting the CBA value from the regional anomaly.

Derivative Analysis

The Second Vertical Derivative (SVD) method exhibits high-pass filter properties, which were utilized to remove shallow effects, clarify the structure, and delineate boundaries. SVD Bouguer anomaly with a value of zero (0) can indicate a significant change in density, in the form of faults, anomalous object boundaries, lithology boundaries, and basin boundaries [24]. The Second Vertical Derivative (SVD) analysis process utilized the Henderson & Zietz (1949) [25], Elkins (1951) [26], and Rosenbach (1953) [27] operators implemented in Surfer 13 software. SVD is the result of deriving the Laplace equation from the gravity anomaly on the Earth's surface [28]:

$$\frac{\partial^2 \Delta g}{\partial z^2} = -\frac{\partial^2 \Delta g}{\partial x^2} + \frac{\partial^2 \Delta g}{\partial y^2} \quad (2)$$

where:

∇^2 : Laplace operator
Δg : total gravity Bouguer value
∂y : y-axis derivative value
∂x : x-axis derivative value

In addition to strengthening the results of the structure delineation based on the SVD analysis, a horizontal gradient analysis was used. The First Horizontal Derivative (FHD) method emphasizes the maximum and minimum peak value information in the anomaly data to show the boundaries of the geological structure causing the anomaly. The FHD value can be calculated using Equation 3 [29].

$$FHD = \frac{\Delta g}{\Delta x} = \frac{g_{(i+1)} - g_{(i)}}{\Delta x} \quad (3)$$

The Second Horizontal Derivative (SHD) method reveals the presence of geological structure boundaries, as indicated by zero boundary information in the SHD value.

$$SHD = \frac{\Delta g}{\Delta x} = \frac{2g_{(i+1)} - 2_{(i)}}{\Delta x^2} \quad (4)$$

Inversion Modeling

3D Inversion Modeling is backward modeling (inverse modeling). The data used in 3D inversion modeling were the gravity anomaly data, topography data, and mesh data. Inversion modeling was employed to model the distribution of anomalous density, thereby enhancing the interpretation of the structure and existence of reservoir prospects, cap rocks, and heat sources in the research area.

RESULTS AND DISCUSSION

Results

The complete Bouguer Anomaly map in the research area shows that the range of anomaly values is between 150 and 230 mGal (Figure 6). Lower anomaly values ranging from 150 mGal to 175 mGal are distributed in the northeast of the research area. Medium anomaly values range from 180–195 mGal. Meanwhile, high anomaly values range from -200 to 230 mGal, reflecting the high-density distribution resulting from volcanic products of Mount Patuha. The density variation of the Complete Bouguer Anomaly value exhibits a correlation with the Patuha structural pattern (see Figure 4).

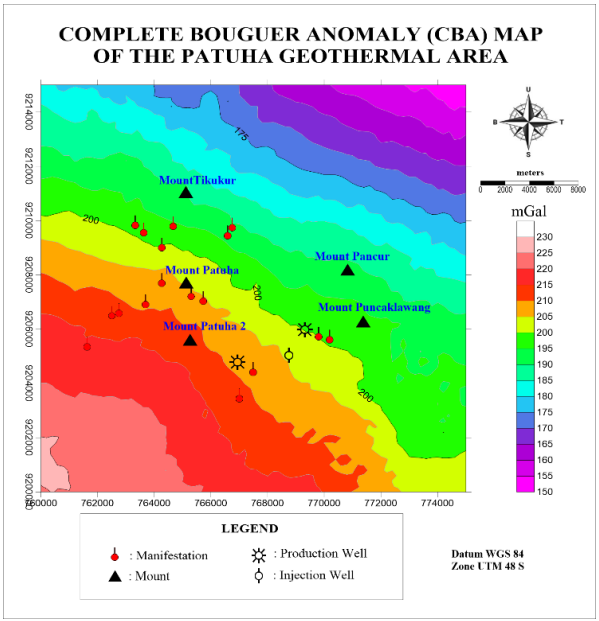

Figure 6. Complete Bouguer anomaly map of the Patuha geothermal area

The high-density area is located in the southwest area, corresponding to the lava and lahar formations of Mount Patuha. This area is composed of tuff and breccia formations, which are types of volcanic rocks. This high-density area is also influenced by the fact that the area is located closest to the subduction zone and experiences volcanic activity, in contrast to the area in the northeast, which has low density and is dominated by reef limestone formations.

Spectrum analysis was carried out to obtain the cut-off value (k_c) by plotting the wave number and ln A values. The cut-off value (k_c) is the boundary between the regional anomaly and the residual anomaly. This spectrum analysis was also conducted to determine the optimal window width value for separating regional anomalies from residual anomalies using a moving average filter (Tables 1 and 2).

Table 1. Regional and residual anomaly depth

Line	Regional depth (m)	Residual depth (m)
Line 1	-4840.8	-418.42
Line 2	-4520.8	-412.31
Line 3	-5430.7	-351.17
Line 4	-5424.3	-427.34
Line 5	-5918.7	-515.25
Average	**-5227.06**	**-424.898**

Table 2. Cut off value (k_c) and window width (N)

Line	Cut Off (k_c)	Window Width (N)
Line 1	0.000795	39.54
Line 2	0.000823	38.16
Line 3	0.000848	37.05
Line 4	0.000793	39.63
Line 5	0.000599	52.45
Average	**0.000771**	**41.37**

The regional anomaly contour map displays a range of low to high anomaly values, ranging from 155 to 225 mGal (Figure 7). The low anomaly value is within the range of 155 to 175 mGal, located in the northeast to north of the research area map. The range of medium anomaly values is between 180 and 195 mGal, located from east to northwest of the research area map. The high anomaly value has a range of 200 to 225 mGal, which is in the southwest of the map.

p-ISSN 0854-1418
e-ISSN 2503-426X

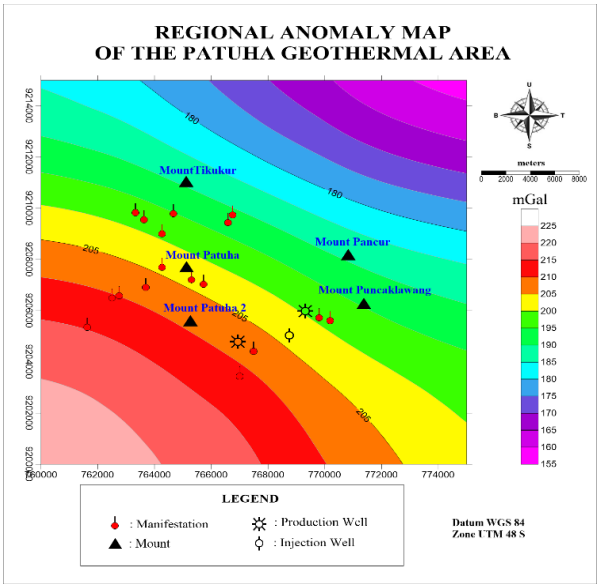

Figure 7. Regional anomaly map of the Patuha geothermal area

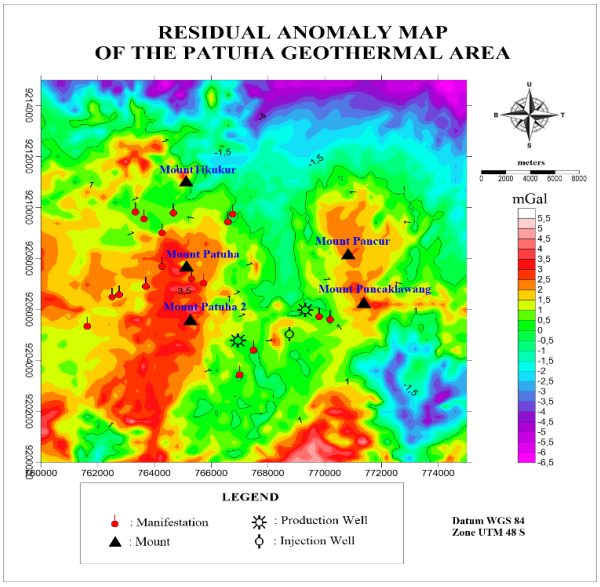

Figure 8. Residual anomaly map of the Patuha geothermal area

Residual anomalies are anomalies with high-frequency values, which result from the smaller area coverage and are caused by local geological structures or small geological features. The varying density distribution in the residual anomaly is caused by the presence of different rock types at shallow depths. High density is found in areas around mountains caused by volcanic activity, resulting in high density in shallow areas.

The residual anomaly map spans a range of low to high anomaly values (Figure 8). The range of low anomaly values is from -6.5 mGal to -3 mGal, which dominates the northern part of the map, stretching from northwest to northeast. The moderate anomaly value ranges from -2.5 mGal to 0.5 mGal, which dominates the map of the research area. While the high anomaly value is in the range of 1 to 5.5 mGal, there are Mount Pancur, Mount Puncaklawang, Mount Tikukur, Mount Patuha 1, and Mount Patuha 2 with high anomaly values.

The anomaly value on the SVD map ranges from -7 to 6 mGal/m² (Figure 9). The low anomaly value ranges from -7 to -1 mGal/m², which is distributed across the northern part of the area. The medium anomaly value ranges from -0.5 to 1.5 mGal/m². In comparison, the high anomaly value dominates the research area, as indicated by anomaly values ranging from 2 to 6 mGal/m². The thick black line on the map is the anomaly contour value of 0 mGal/m^2. The solid and dashed purple line is the fault structure from the geological map and geothermal manifestation map of the Patuha field. The white lines are identified fault structures (Figure 10).

Based on the results of 3D inversion modeling (Figure 11), residual anomaly data indicate a density range of 2 to 3 g/cm³. The Patuha reservoir prospect is estimated to be among the high anomaly (at a density of 2.5 g/cc), precisely near the heat source. A density value of 2.66 g/cc can be indicated as the location of the cap rock, which is located in a shallow area above the reservoir. In comparison, high anomaly with a value range

of 2.83 g/cc to 3 g/cc can indicate the location of the heat source. The heat source in the Patuha geothermal system is a shallow type of heat source. It originates from magma that has solidified under the Cibuni Crater, White Crater, and Ciwidey Crater.

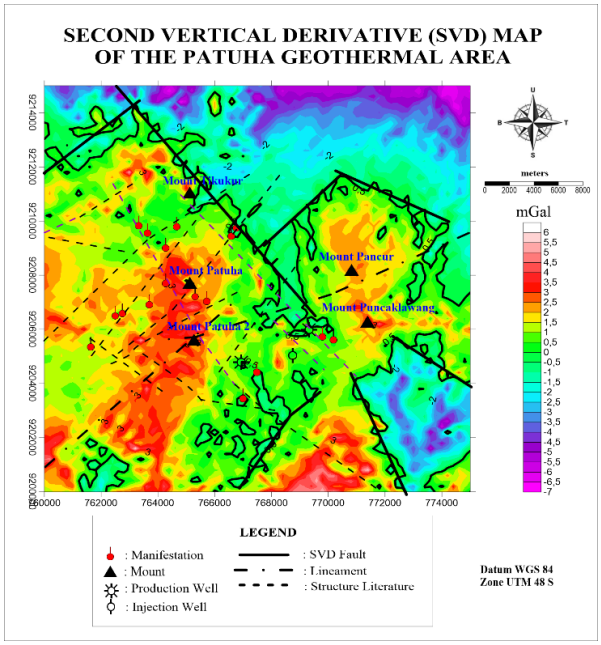

Figure 9. Second vertical derivative map of Patuha geothermal area (literature structure, [21])

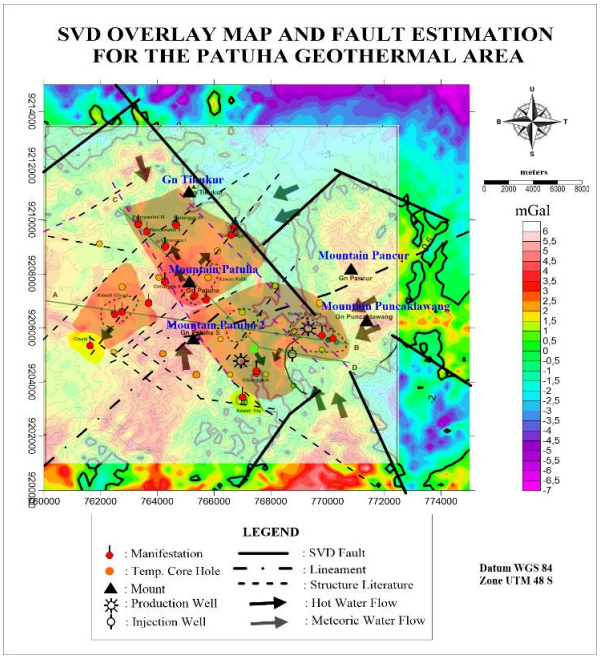

Figure 10. SVD overlay map and fault estimation of the Patuha geothermal area

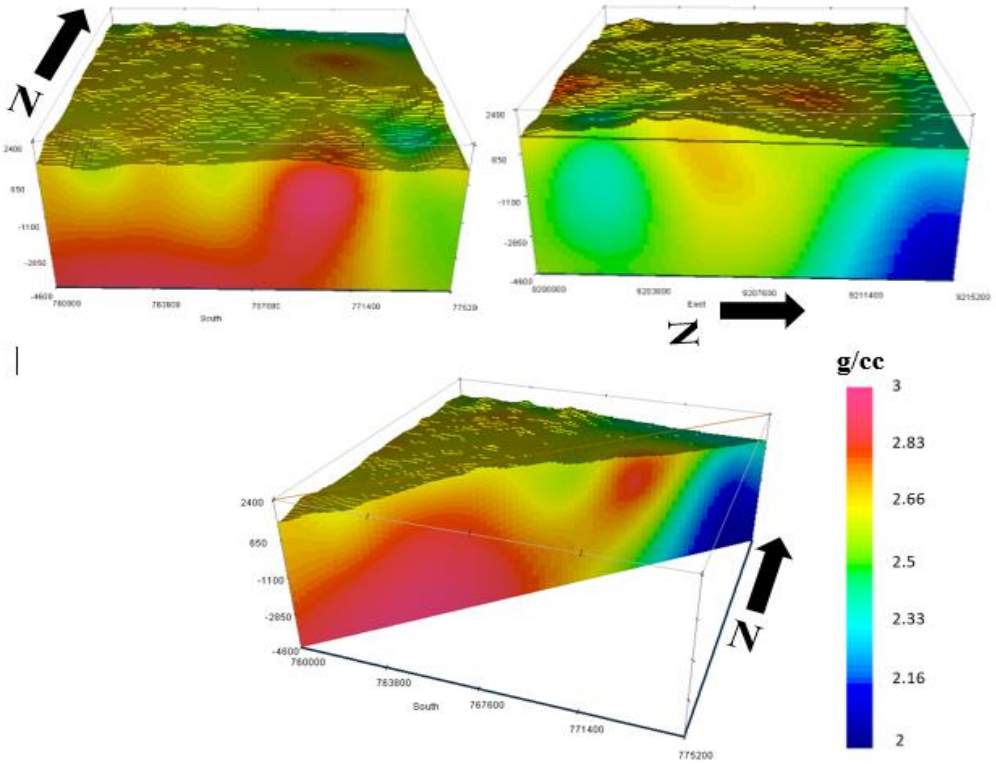

Figure 11. The density distribution model results from the 3D inversion modelling of the residual Bouguer anomaly

p-ISSN 0854-1418
e-ISSN 2503-426X

Discussion

The A-A' cross-section line (760000-774000 mE) reveals the presence of a fault structure, which is interpreted based on the FHD curve (Figure 12). The FHD curve exhibits maximum and minimum absolute values, and the SVD/SHD curve reaches a value of 0 mGal/m². The solid black line and the dashed black line are identified as faults because they are at a value of 0 mGal/m^2 and are at the maximum and minimum absolute values of the wave, and show a contrast in density changes. The dashed black line is identified as a normal fault, marked by the maximum absolute value on the SVD/SHD curve being greater than the minimum absolute value. The solid black line is identified as a reverse fault, marked by the minimum absolute value on the SVD/SHD curve being greater than the maximum absolute value. The A-A' line intersects the manifestation, the PPL-6ST Production Well, and Mount Patuha 2. A graben structure was formed in the Patuha Field due to the presence of adjacent downthrust fault structures, causing depression (subsidence). The graben structure is located in the reservoir area, which also serves as the outlet for the manifested fluid.

The reservoir in the Patuha geothermal system is located directly below the manifestation and the PPL-6ST Production Well. It can be observed that the manifestation fluid that emerges on the surface is influenced by the presence of a graben structure, specifically a normal fault. The Patuha Field reservoir has a density of 2.5 g/cc, marked in green, located at a depth of 1800 meters above mean sea level (MSL) to 900 meters below MSL, with a length of approximately 2 km. The cap rock is located directly above the reservoir and the heat source. Cap rock on this track has a density of 2.66 g/cc, marked in yellow; cap rock is at a depth of 2300 meters above MSL to 400 meters below, which spreads about 10 km. At the same time, the heat source in the Patuha Field is located directly below the Cibuni Crater, with a density of around 3 g/cc marked in purple, at a depth of 200 to 4600 meters below MSL.

The B-B' line intersects the PPL-6ST Production Well and the PPL-1A Injection Well. A graben structure is present in the reservoir area, characterized by two main normal fault structures (Figure 13). The geothermal reservoir is located directly below the PPL-6ST Production Well and the PPL-1A Injection Well. The Patuha Field Reservoir has a density of 2.5 g/cc, marked in green, which is at a depth of 1800 meters above MSL to 1000 meters below MSL and extends about 2 km. The cap rock is located directly above the reservoir and has a density of 2.66 g/cc, marked in yellow. The cap rock is at a depth of 2200 meters above MSL to 0 meters MSL, which spans about 4.2 km. Meanwhile, the heat source is located under the Patuha Field reservoir with a density of around 3 g/cc, which is marked with purple at a depth of 300 to 4600 meters below MSL.

The C-C' line intersects the PPL-3B Production Well and the manifestation. There is a graben structure that intersects the reservoir, and the intersection is the exit path for the manifested fluid to the surface (Figure 14). In the graben area, there are indications of magma intrusion, as indicated by high to low density, which is near the manifestation. The reservoir in the Patuha geothermal system is located directly below the PPL-3B Production Well. The Patuha Field Reservoir has a density of 2.5 g/cc, which is marked in green, at a depth of 1900 meters to 900 meters above MSL, with a length of about 2 km. The cap rock is located directly above the reservoir, has a density of 2.66 g/cm³, and is marked in yellow. Cap rock is at a depth of 2200 meters

to 300 meters above MSL, which spans about 3.2 km. Meanwhile, the heat source in the Patuha Field is identified as coming from the volcanic activity of Mount Patuha, indicated by the heat source located directly below it. The heat source has a density of around 3 g/cc, which is marked with purple at a depth of 0 to 4600 meters below MSL.

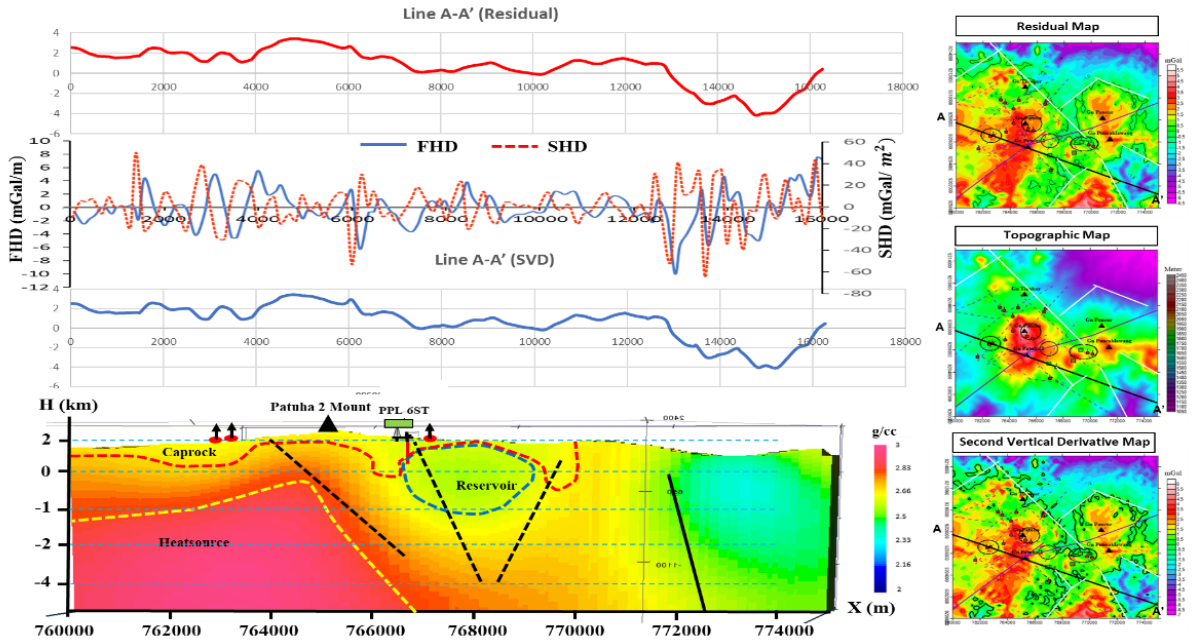

Figure 12. Cross-section of line A-A'

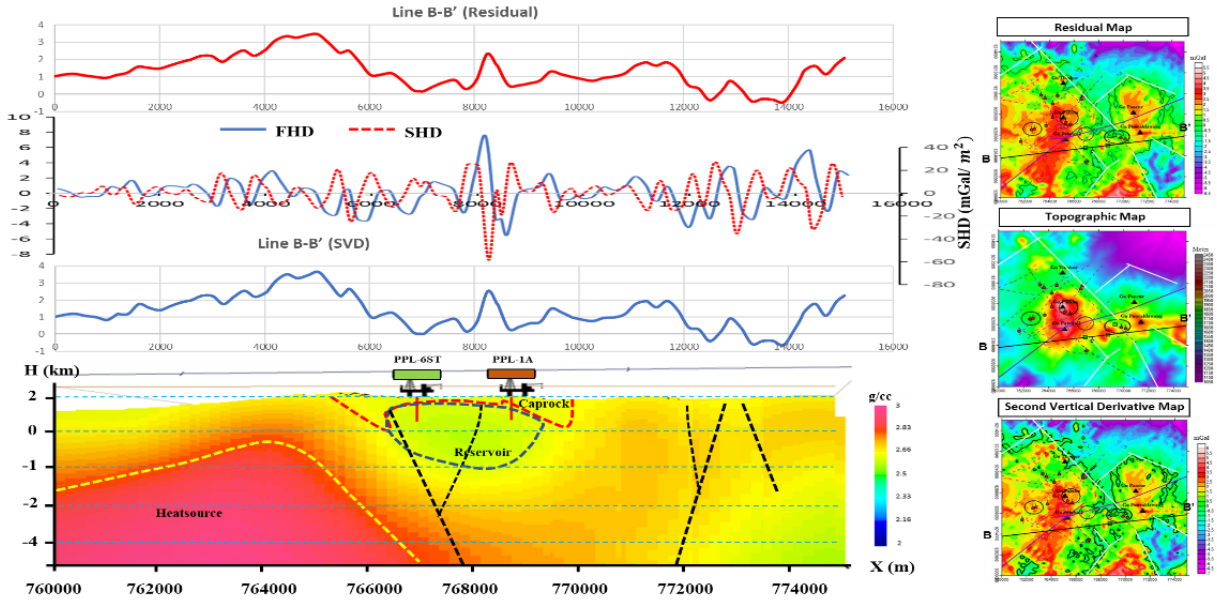

Figure 13. Cross-section of line B-B

p-ISSN 0854-1418
e-ISSN 2503-426X

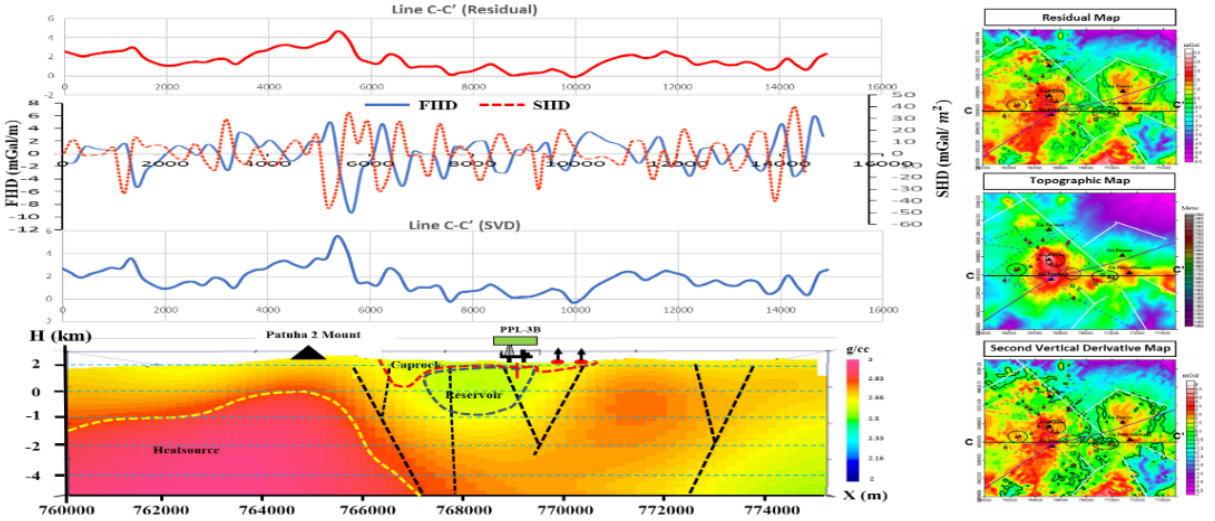

Figure 14. Cross-section of line C-C'

The D-D' line intersects the PPL-3B Production Well. There is a thrust fault on the left side of the well and a thrust fault on the right side of the well (Figure 15). The geothermal reservoir is located directly below the PPL-3B Production Well. The Patuha Field Reservoir has a density of 2.5 g/cc marked in green, which is located at a depth of 1800 meters above MSL to a depth of 1300 meters below MSL with a length of about 5.2 km. The Cap rock is located directly above the reservoir, with a density of 2.66 g/cc, marked in yellow. It spans a depth of about 2200 meters to 700 meters above MSL, covering an area of about 7.3 km.

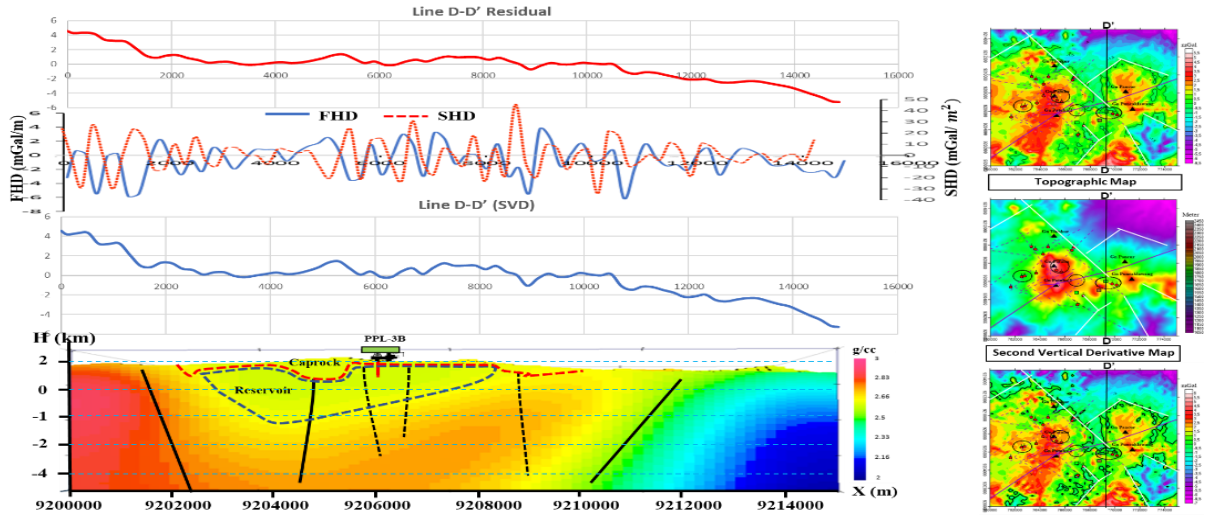

Figure 15. Cross-section of line D-D'

The E-E' line intersects the PPL-6ST Production Well and manifestation. A graben structure is present in the reservoir prospect area, with the main structure characterized by a normal fault (Figure 16). The reservoir in the Patuha geothermal system is located directly below the manifestation. It can be observed that the fluid that manifests on the surface

originates from the downward fault path that intersects the reservoir. The Patuha Field Reservoir has a density of 2.5 g/cc, marked in green at a depth of 1800 meters to 900 meters above MSL with a length of about 3.5 km. The cap rock is located directly above the reservoir and the heat source, with a density of 2.66 g/cc, is marked in yellow at a depth of about 2200 meters to 1400 meters above MSL, which spreads about 7.8 km. In contrast, the heat source has a density of around 3 g/cc, which is marked in purple, located at a depth of 3800 meters to 4600 meters below MSL.

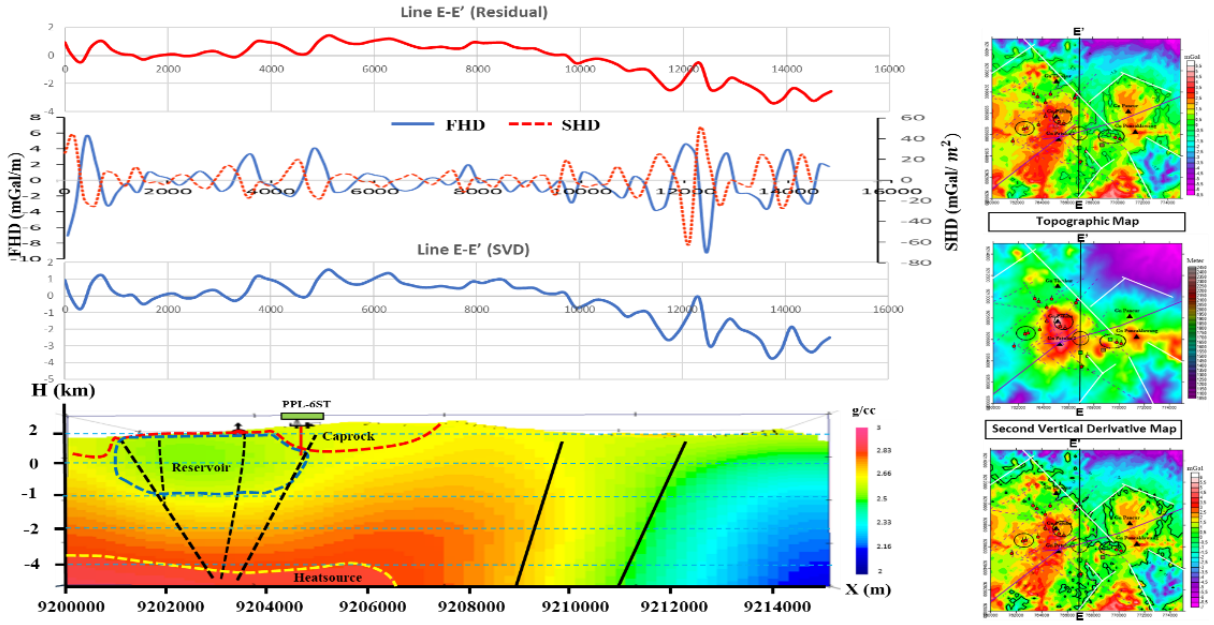

Figure 16. Cross-section of line E-E'

The F-F' line intersects the PPL-3B Production Well, the PPL-1A Injection Well, and Mount Pancur. The graben structure is located in the reservoir area, characterized by a main structure in the form of a normal fault. The graben structure intersects the reservoir, making it the fluid outlet to the PPL-3B Production Well. The reservoir in the Patuha geothermal system is located directly below the PPL-3B Production Well and the PPL-1A Injection Well. The existence of a fault in the graben structure serves as an outlet for the fluid produced by the PPL-3B Well. The Patuha Field Reservoir has a density of 2.5 g/cc, which is marked in green, and has a depth of 2100 meters above MSL to 900 meters below MSL, which extends about 4 km. Cap rock is located right above the reservoir with a density of 2.66 g/cc, marked in yellow at a depth of about 2200 meters to 400 meters above MSL, which spreads about 6.2 km. The grey line below Mount Pancur is identified as a magma intrusion, in line with the presence of high to low density in the area. The magma intrusion is closely related to the presence of a heat source.

p-ISSN 0854-1418
e-ISSN 2503-426X

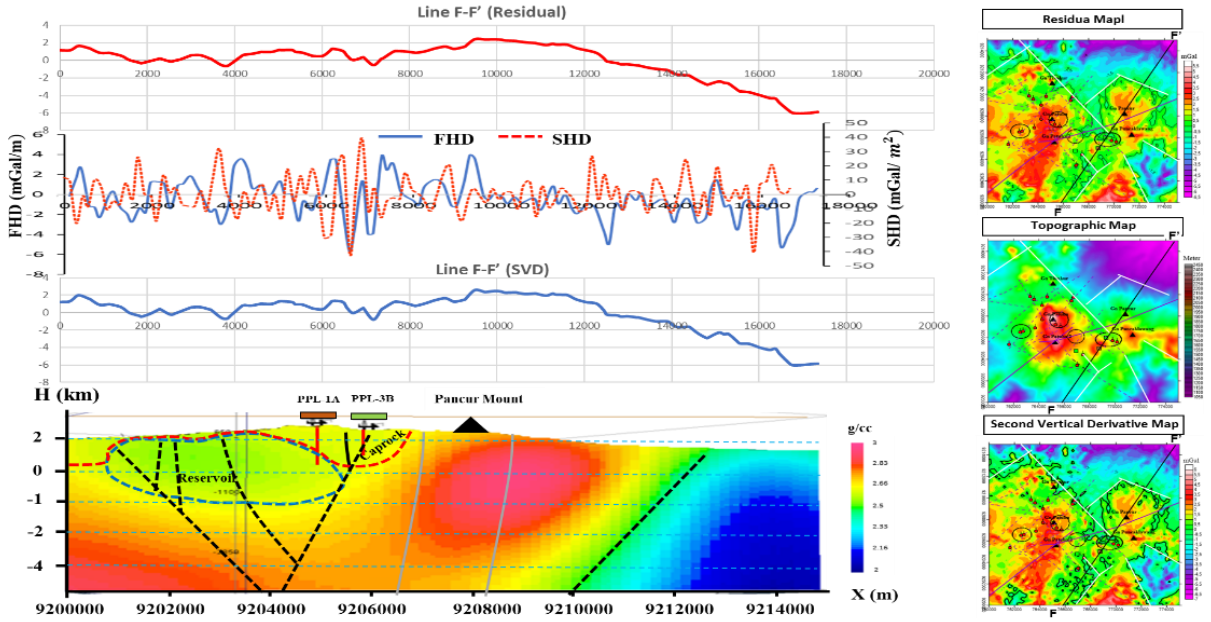

Figure 17. Cross-section of track F-F'

The gravity data indicate that the reservoir boundary has a wider prospect when viewed from the structural boundary, with a value of 0 mmGal/m². According to the Patuha geothermal area map, the reservoir boundary covers an area of approximately 63 km². The SVD structural boundary shows that the Patuha area reservoir has an area of approximately 130 km^2 (Figure 18). Meanwhile, based on MT data (1250 MASL), the reservoir boundary has an area of approximately 42 km^2 (Figure 19).

Differences in capabilities between the MT method and the gravity method result in a difference in reservoir area (Figure 20). MT is very effective at identifying conductive layers, such as clay caps and fluid zones. Still, the resistivity of hot fluids can be complex, sometimes not contrasting enough with its surroundings to be detected as a reservoir [30].

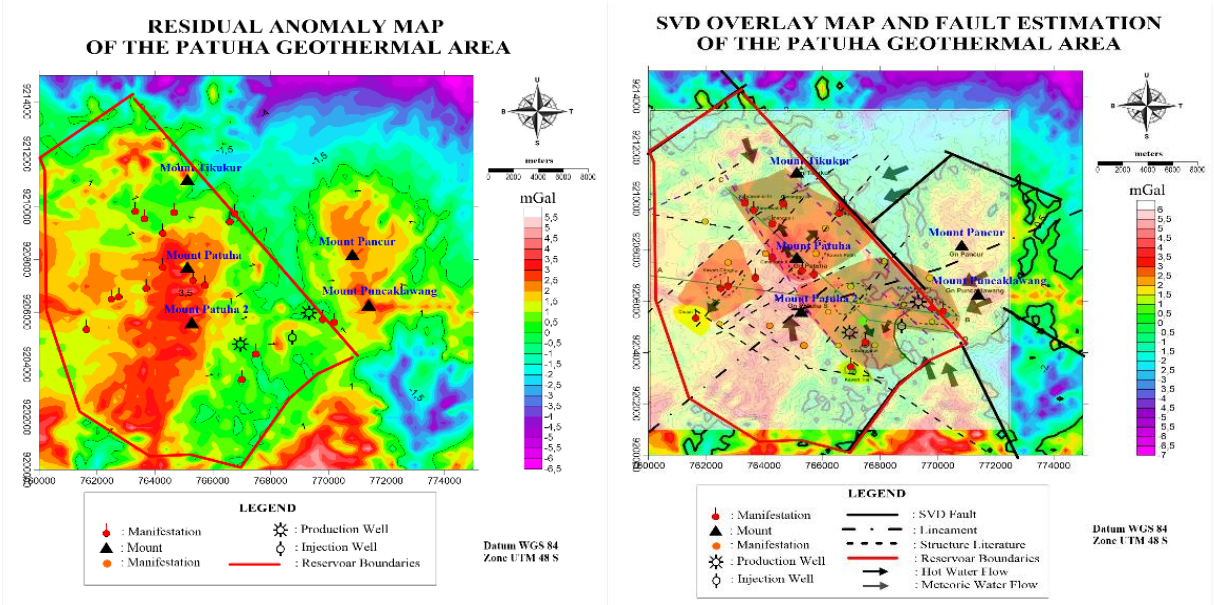

Figure 18. Comparison between the reservoir boundary of the Patuha field (left) and the SVD Patuha geothermal area map (right).

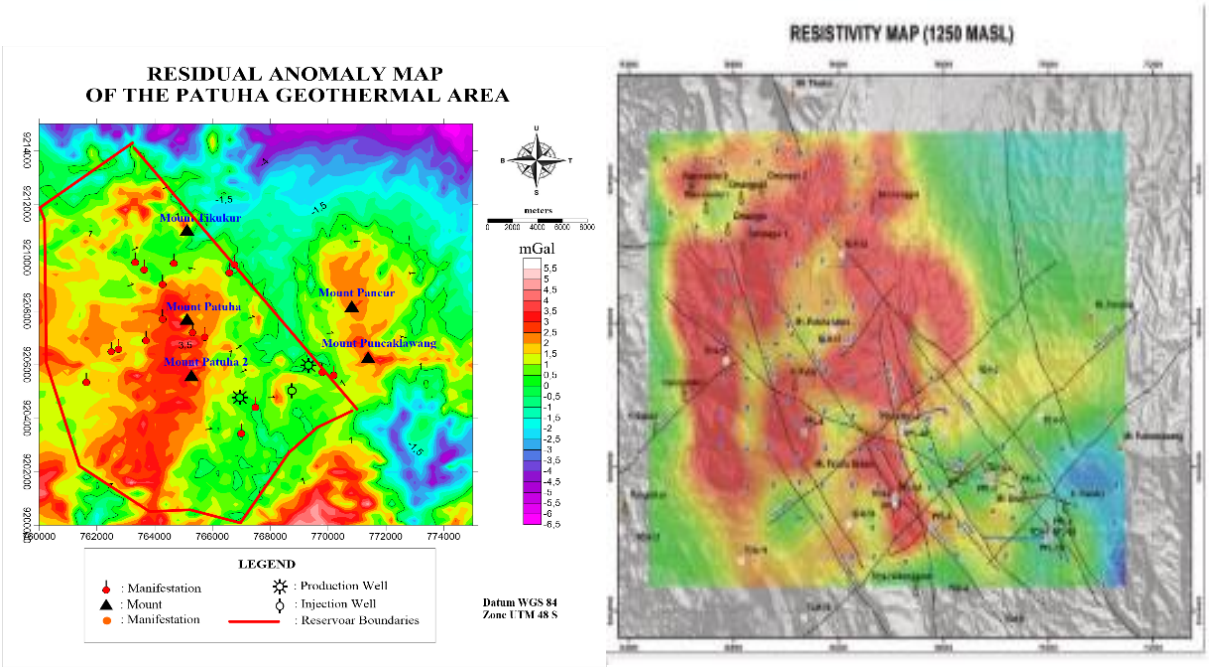

Figure 19. Comparison between the Patuha field reservoir boundary (left) and the MT map at 1250 MASL [32] (right)

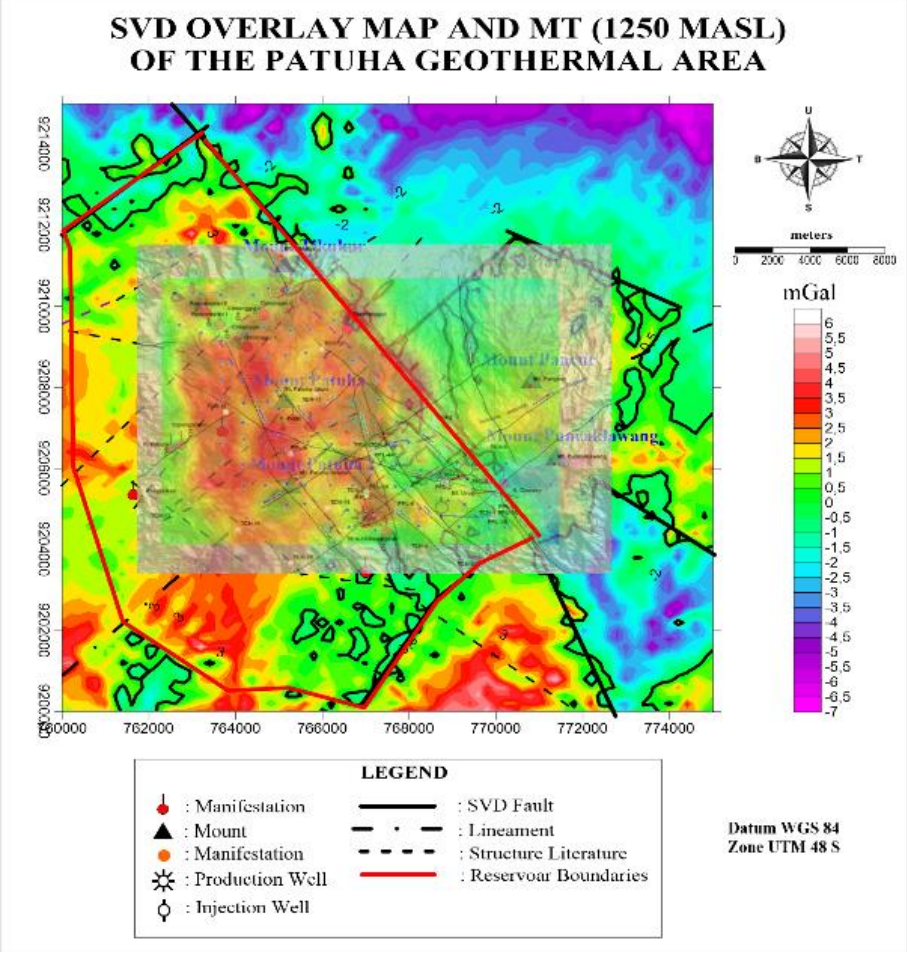

Figure 20. Reservoir boundary of Patuha Field overlain by SVD and MT map 1250 MASL [32]

p-ISSN 0854-1418
e-ISSN 2503-426X

The differences in gravitational field measurements are determined by rock mass and depth of sources/structures. The surface-gravity technique can be applied to any field, depending on reservoir thickness, size, depth, porosity, and density contrast between the fluids. Rock and fluid density contrasts determine the response [31].

When slicing is carried out on cutting production wells, injection wells, and manifestations, it can be concluded that the geothermal reservoir prospects that have been developed are in the Ciwidey Crater. The reservoir is at a depth of around 2200 meters above MSL to 700 meters below MSL. Based on the Magnetotelluric Method modeling, the reservoir is at a depth of 1500 meters above MSL to 1000 meters below MSL, has a moderate resistivity of 200–100 ohm.m, and is near the Cibuni Crater and Ciwidey Crater.

The cap rock in the Patuha geothermal system is a clay cap that extends across the Cibuni Crater, White Crater, and Ciwidey Crater. A cap rock (clay cap) is a rock with low porosity and permeability, and its function is to protect heat energy and reservoir fluids. The existence of cap rock between the White Crater and the Ciwidey Crater is supported by MT data, indicating a low-resistivity zone in the area between the White Crater and the Ciwidey Crater. The Patuha Field cap rock (clay cap) is at a depth of 2300 meters to 800 meters above MSL. Based on the Magnetotelluric Method modeling literature, cap rock (clay cap) is at a low resistivity, namely (<15 ohm.m), which is at a depth of 1500 meters above MSL to 500 meters below MSL, which also extends across the Cibuni, White, and Ciwidey Crater.

The Patuha geothermal heat source is closely related to the volcanic activity of Mount Patuha (Kawah Putih). The heat source, located near the surface and close to the reservoir, causes the reservoir temperature to be high, resulting in a steam-dominated geothermal system [19]. Based on the modelling results, the heat source was identified as being located right under the Cibuni Crater, with a depth of 1500 meters above MSL to 4600 meters below MSL. The heat source is indicated to be magma that has solidified and undergone a heat release process (cooling). Based on MT modelling, the heat source has a resistivity value of greater than 500 ohm.m at elevations below 0 m MSL, which is located below the Cibuni Crater and Ciwidey Crater. In addition, right under the White Crater, there is an indication of the presence of magmatic substances flowing in the area, causing the fluid to be acidic.

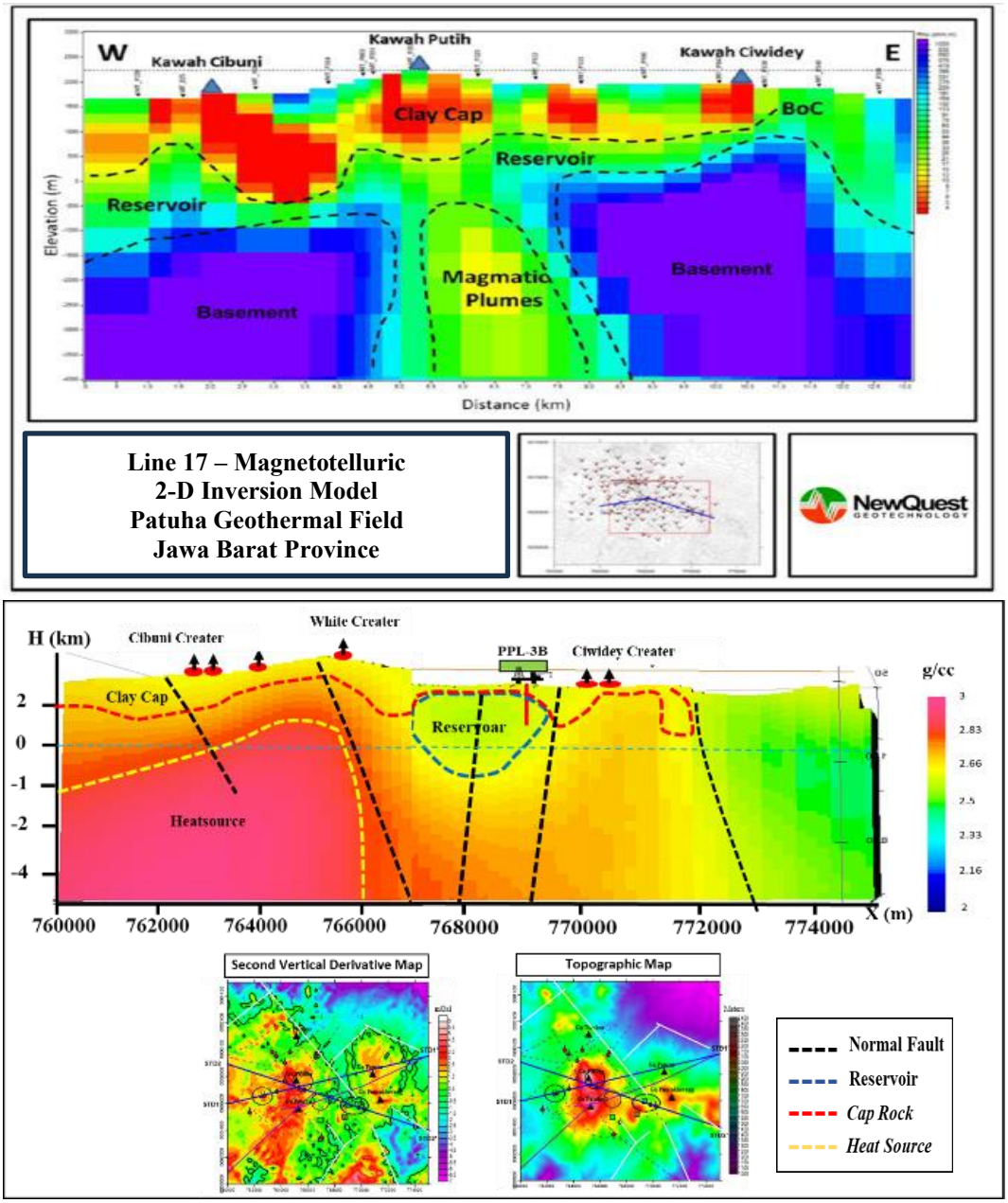

Figure 21. Interpretation of the Patuha geothermal system model based on gravity modeling analysis supported by MT data [10]

CONCLUSION

3D inversion modeling of the gravity anomaly reveals the distribution of density both laterally and vertically, extending to a depth of 4600 meters. The density value obtained, with a range of 2 to 3 g/cm³, represents the density of the rocks in the study area. The modeling results indicate that the Patuha geothermal reservoir prospect lies between the White Crater and the Ciwidey Crater, which is controlled by a graben structure formed due to extensional forces. The reservoir boundary overlaid with the SVD map has an area of approximately 130 km^2 and is at a depth of approximately 2200 meters above MSL to 700 meters below MSL. In the MT model, the reservoir is located in the Cibuni Crater and Ciwidey Crater areas. Clay caps along the Cibuni Crater, White Crater, and Ciwidey Crater, supported by MT data, are

p-ISSN 0854-1418
e-ISSN 2503-426X

at a depth of 2300 meters to 800 meters above MSL. The heat source in the Patuha Field is close to the surface. It is under the Cibuni Crater (sourced from under Mount Patuha) at a depth of 1500 meters above MSL to 4600 meters below MSL. The Ciwidey crater area shows a high anomaly contrast influenced by the volcanic activity of Mount Patuha. However, due to the limited availability of GGMPlus satellite data, the heat source in the Ciwidey crater does not yet exhibit a definite density contrast. In the MT model, the heat source is located under the Cibuni Crater and Ciwidey Crater.

ACKNOWLEDGMENT

Thank you to all parties involved and those who contributed to the research.

REFERENCES

[1] S. Broto and T. T. Putranto, "Aplikasi Metode Geomagnet dalam Eksplorasi Panasbumi," *Teknik*, vol. 32, no. 1, pp. 79–87, 2011, doi: 10.14710/teknik.v32i1.1687.

[2] S. J. Zarrouk and K. McLean, *Geothermal Well Test Analysis*, 2019, Elsevier, doi: 10.1016/c2017-0-02723-4.

[3] M. F. Khasmadin and U. Harmoko, "Kajian Potensi dan Pemanfaatan Energi Panas Bumi di Wilayah Kerja Panas Bumi Patuha Ciwidey," *J. Energi Baru dan Terbarukan*, vol. 2, no. 2, pp. 101–113, 2021, doi: 10.14710/jebt.2021.11187.

[4] B. Suranta, V. Wenov, A. Sofyan, and H. Aka, "Estimasi Potensi Sumber Daya Panasbumi Menggunakan Metode Volumetrik di Lapangan Patuha," *Indones. J. Energy*, vol. 1, no. December 2020, pp. 37–44, 2020.

[5] W. M. Telford, L. P. Geldart, and R. E. Sherrif, *Applied Geophysics*, London: Cambridge University Press, 1990.

[6] M. Sarkowi and R. C. Wibowo, "Reservoir Identification of Bac-Man Geothermal Field Based on Gravity Anomaly Analysis and Modeling," *J. Appl. Sci. Eng*., vol. 25, no. 2, pp. 329–338, 2022, doi: 10.6180/jase.202204_25(2).0009.

[7] M. Sarkowi, R. C. Wibowo, R. F. Sawitri, and B. S. Mulyanto, "Wai Selabung Geothermal Reservoir Analysis Based on Gravity Method," *J. Ilm. Pendidik. Fis. Al-Biruni*, vol. 10, no. 2, pp. 211–229, 2021, doi: 10.24042/jipfalbiruni.v10i2.9705.

[8] C. Hirt, S. Claessens, T. Fecher, M. Kuhn, R. Pail, and M. Rexer, "New Ultrahigh-Resolution Picture of Earth's Gravity Field," *Geophys. Res. Lett*., vol. 40, no. 16, pp. 4279–4283, 2013, doi: 10.1002/grl.50838.

[9] B. Sudrajad, "Pemodelan Struktur Bawah Permukaan Wilayah Kabupaten Nabire di Bagian Utara Leher Burung Pulau Papua Menggunakan Pemodelan Inversi Tiga Dimensi (3D) dan Analisis Horisontal Derivatif Berdasarkan Data Anomali Gravitasi GGMplus," *Tesis*, Universitas Gadjah Mada., 2018.

[10] S. A. Pratama, Y. Daud, F. Fahmi, and C. A. Darusman, "Integrated Analysis of Magnetotelluric and Gravity Data for Delineating Reservoir Zone at Patuha Geothermal Field, West Java," *Proc. Indones. Int. Geotherm. Conv. Exhib*., pp. 1–7, 2015.

[11] I. Setiadi, A. Diyanti and N. D. Ardi, "Interpretasi Struktur Geologi Bawah Permukaan Daerah Leuwidamar Berdasarkan Analisis Spektral Data Gaya Berat," *Jurnal Geologi dan Sumberdaya Mineral*, vol. 15, no. 4, pp. 205–214, 2014, doi: 10.33332/jgsm.geologi.v15i4.59.

[12] S. F. Hidayat, "Penyelidikan Gaya Berat Untuk Pemetaan Struktur Bawah Permukaan di Daerah Karanganyar Bagian Barat," Universitas Sebelas Maret, 2011.

[13] N. A. Rahima, "Studi Pemodelan Struktur Bawah Permukaan menggunakan Metode Gaya Berat di Daerah panas Bumi Kec. Lasusua kab. Kolaka Utara," UIN Alauddin Makassar, 2020.

[14] Badan Informasi Geospasial, "Shapefile Geologi Seluruh Indonesia." [Online]. Available: https://www.indonesia-geospasial.com.

[15] T. Purwantoro, A. Rachman, and M. Silaban, "Potensi dan rencana pengembangan lapangan panas bumi Patuha Jawa Barat," *Proceedings of the 39th IAGI Annu. Conv. Exhib*., 2010.

[16] W. Hamilton, *Tectonics of the Indonesian Region*, United States Geol. Surv. Prof. Pap., no. 1078, 1979.

[17] Badan Informasi Geospasial, "DEMNAS." [Online]. Available: https://tanahair.indonesia.go.id.

[18] GeoMap, "Lembar Geologi Jawa Barat." [Online]. Available: https://geologi.esdm.go.id/geomap/pages/preview/peta-geologi-lembar-cianjur-jawa.

[19] N. M. Saptaji, *Teknik Geothermal*, Bandung: ITB Press, 2020.

[20] E. Layman and S. Soemarinda, "The Patuha Vapor-Dominated Resource West Java, Indonesia," *Proc. 28th Work. Geotherm. Reserv. Eng. (p. SGP-TR173)*, 2003.

[21] A. Ashat and H. B. Pratama, "Application of Experimental Design in Geothermal Resources Assessment of Ciwidey-Patuha, West Java, Indonesia," *IOP Conf. Ser. Eart. Environ. Sci.*, vol. 103, 2017, doi: 10.1088/1755-1315/103/1/012009.

[22] Martodjojo, *Evolusi Cekungan Bogor*, Bandung: Institut Teknologi Bandung, 1984.

[23] M. Nursalam, "Analisis Sesar dengan Data Gayaberat Menggunakan Metode SVD (Second Vertical Derivative) di Daerah Panas Bumi 'MN,'" Universitas Hasanuddin, 2021.

[24] P. Sumintadireja, D. Dahrin, and H. Grandis, "A Note on the Use of the Second Vertical Derivative (SVD) of Gravity Data with Reference to Indonesian Cases," J. Eng. Technol. Sci, vol. 50, pp. 127–139, 2018, doi: 10.5614/j.eng.technol.sci.2018.50.1.9.

[25] R. G. Henderson and I. Zietz, "The Computation of Second Vertical Derivative of Geomagnetic Fields," *Geophys. J.*, vol. 14, no. 4, pp. 508-516, 1949, doi: 10.1190/1.1437558.

[26] T. A. Elkins, "The Second Derivative Method of Gravity Interpretation," *Geophys. J.*, vol. 16, no. 1, pp. 29-50, 1951, doi: 10.1190/1.1437648.

[27] O. Rosenbach, "A Contribution to The Computation of The Second Derivative From Gravity Data," *Geophys. J.*, vol. 18, pp. 894-907, 1953, doi: 10.1190/1.1437943.

[28] M. Sarkowi, "Identifikasi Struktur Daerah Panas Bumi Ulubelu Berdasarkan Analisa Data SVD Anomali Bouguer," *J. Sains MIPA*, vol. 16, no. 2, 2010, [Online]. Available: http://repository.lppm.unila.ac.id/id/eprint/22328.

[29] R. Blakely, *Potential Theory in Gravity and Magnetic Applications*, Cambridge University Press, 1996.

[30] B. Oskooi and S. M. Ansari, "Application of Magnetotelluric Method in Exploration of Geothermal Reservoirs with an Example from Iceland," *J. Earth Sp. Phys.*, vol. 37, no. 4, pp. 93-106, 2012, doi: 10.22059/jesphys.2012.24304.

[31] P. Soupios, S. Kaka, P. Kirmizakis, and M. Tranos, "Characterizing and Monitoring an Oil/Geothermal Reservoir using Non-seismic (Integrated CSEM, Gravity Surveys and Microseismic Surveys) Methods," *College of Petroleum Engineering & Geoscience, King Fahd University of Petroleum & Minerals,* [Online]. Available: cpg-webmaster@kfupm.edu.sa, [Accessed: Jul. 17, 2025].

[32] C. Iskandar and Y. Daud, "The Correlation Between 3-D Magnetotelluric Inversion Model with Drilling Data in Patuha Geothermal Field," Bul. Sumber Daya Geol., vol. 17, no. 1, pp. 51–64, 2022, doi: 10.47599/bsdg.v17i1.328.